A 585 GHz Quasi-Optical HEB Six-Port Reflectometer Based on an Annular Slot Antenna

R. Percy, L. Liu, H. Xu, J. Schultz, A.W. Lichtenberger, R.M. Weikle, II
Charles L. Brown Department of Electrical and Computer Engineering
University of Virginia, Charlottesville, VA 22904, U.S.A.
* Contact: rrp4d@virginia.edu, phone +1-434-924-6575

Abstract — **Six-port reflectometers have become a topic of interest due to the scarcity of instrumentation for measuring scattering parameters (s-parameters) at terahertz frequencies. This paper presents a quasi-optical six-port reflectometer designed for 585 GHz using hot-electron bolometers (HEB's). In this design, a ring slot antenna couples a signal into the reflectometer creating a standing wave along a microstrip transmission line. The standing wave is sampled by three evenly spaced HEB's. A polarization rotation resulting from the feed of the transmission line allows the antenna to act as both the input and measurement ports (horizontally polarized energy is coupled into the device and re-radiated with vertical polarization). The reflectometer is expected to be sensitive to nanowatt power levels from 570 GHz to 640 GHz. The annular slot antenna and microstrip portion of the device have been independently fabricated and tested. This proof-of-concept test verifies that the polarization is rotated and provides an estimate of the power available for sampling. It was found that approximately 30 µW of power is available, as measured with an Erickson power meter. Simulations in conjunction with these data indicate that the HEB's should be capable of detecting 100's of nanowatts. This requires each HEB to have approximate dimensions of 100nm by 200nm. This paper presents the six-port design and preliminary measurements.**

I. Introduction

A six-port reflectometer is a compact and relatively inexpensive method for measuring scattering parameters that has outstanding potential for characterizing terahertz components and materials. The realization of such a device at terahertz frequencies would permit diagnostic and measurement capabilities not currently available. Potential uses include characterizing materials such as absorbers, windows, lenses, and other components used in terahertz systems. The six-port reflectometer presented in this work will be realized using three diffusion cooled niobium hot-electron bolometers operating as direct detectors. The input and measurement ports will utilize the antenna using a rotation in the polarization of the signal.

II. Six-port Reflectometers

A six-port reflectometer measures the reflection coefficient of a material using four evenly spaced power detectors [1]. If the device under test is known to be passive, then only three detectors are necessary, resulting in a five-port reflectometer [2]. These detectors sample a standing wave that results from the reflection of a signal on a device under test (DUT). A general representation of a six-port is illustrated in fig. 1. Using various calibration schemes and the ratios of the measured powers, the reflection coefficient for the device can be determined [3].

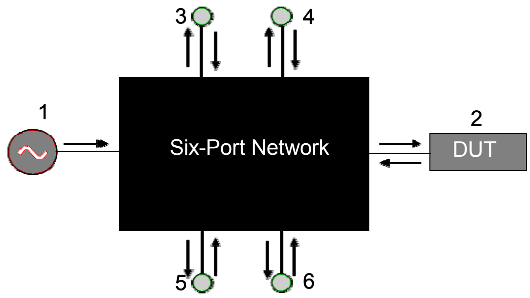

Fig. 1: Representation of a six-port reflectometer. Port 1 is the signal input port, port 2 is the measurement port, and ports 3-6 couple to the power detectors.

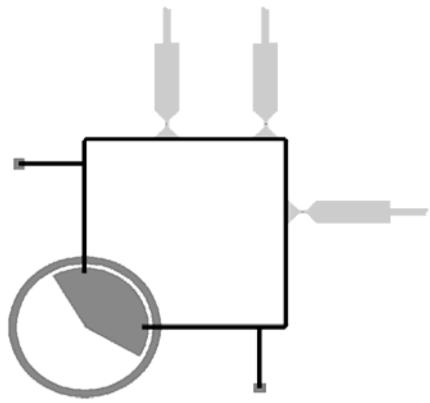

Fig. 2: Prototype submillimeter six-port reflectometer. The ring slow antenna acts as ports 1 and 2 from fig. 1. The detectors at ports 3, 4, and 5, are connected to low pass filters (truncated in this figure). There is a ground pad in the center of the antenna and at the end of each stub.

III. Device Design

A. Polarization

This prototype submillimeter six-port reflectometer utilizes a ring slot antenna to couple both source (port 1) and measurement (port 2) ports (FIGURE # 2). Three hot-electron bolometers (HEB) are used as direct power detectors and are located at ports 3, 4, and 5. A low pass filter follows each HEB to block the RF signal and allow the DC detected response to pass. A fourth detector (port 6) is not necessary for the measurement of passive devices and has not been included. The port numbers in the device schematic (fig. 2) correspond with the port numbers in the general six-port representation (fig. 1).

The use of the antenna as two different ports is achieved by exploiting a change in polarization. An experimental setup (fig. 3) illustrates this idea. The input signal is passed through a polarization grid allowing only one polarization (e.g. – horizontal) to reach the antenna and be coupled into the device as illustrated by the solid arrows. This signal passes through a transmission line with a 90º bend and is re-radiated with the opposite polarization (e.g. – vertical). When this re-radiated signal reaches the polarization grid, it is completely reflected and is directed toward the DUT as shown by dotted arrows. The reflected portion of the signal follows its path back into the six-port (dashed) and creates a standing wave along the transmission line. Three probes along the line allow the HEB's to detect the power at each point.

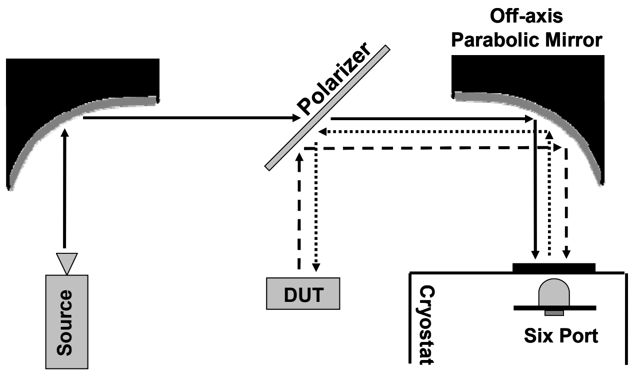

Fig. 3: The experimental setup. The input signal (solid line) is vertically polarized. The output signal (dotted line) is horizontally polarized from the six-port. The signal (dashed line) is the reflection from the DUT.

B. Power Detector Coupling

An important design consideration is the location and size of the probes. Ideally, they are $\lambda/6$ apart so that the standing wave is sampled within a half-wavelength over an octave bandwidth [2]. Another consideration is balancing the power available to each individual HEB and to the output. Two designs have been considered: the first employs a shorted stub tuning network to match the antenna impendence to the microstrip impedance and to provide a ground for the HEB's as (fig. 2); a second uses an open circuited stub matching network and includes separate quarter-wave stubs to ground. The coupling data for the first design is shown in fig. 4 and is similar to that of the second design. These ADS Momentum simulations are used to calculate the amount of power available to each HEB and the size required for the HEB.

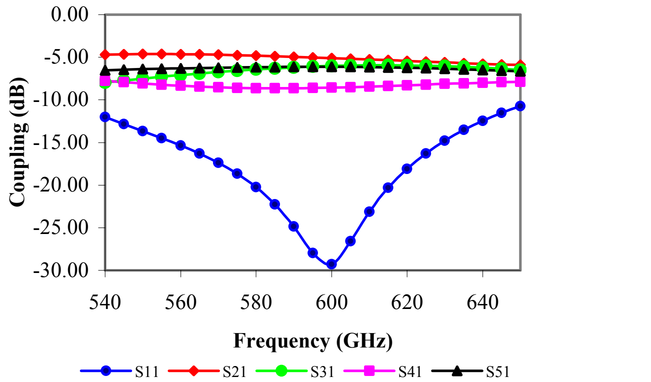

Fig. 4: ADS Momentum simulation of the power in dB coupled into each port for scheme 1. S11 is the input reflection, S21 is the output signal, and S31, S41, and S51 are the ports. Each port is identical with the exception of position showing they are not independent.

C. Power Detectors

The power detectors to be used in this six-port reflectometer are niobium hot-electron bolometers (HEB's). The slope of the R-T curve (fig. 5a) near the superconducting transition for these devices is very sharp, allowing a small change in temperature to change the resistance of the device significantly. Monitoring the I-V curve (fig. 5b) of the bolometer allows the power absorbed to be determined [4]. The sensitivity of an HEB depends on its volume. The devices designed for this application will be 10 nm thick and have area of 100nm x 200nm [5].

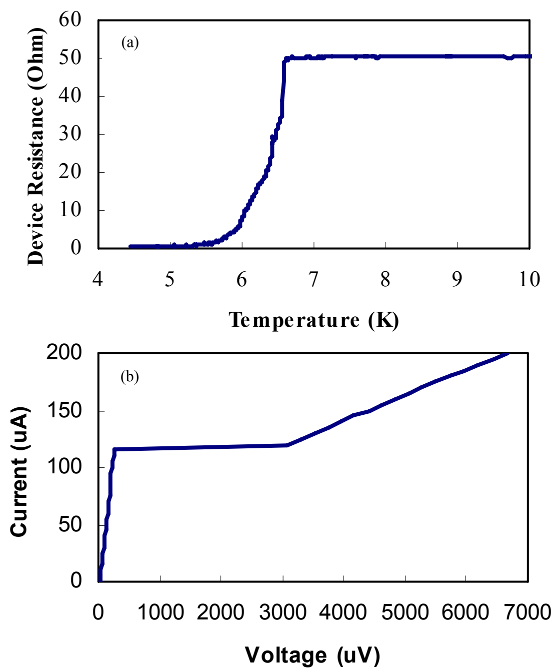

Fig. 5: Typical (a) R-T and (b) I-V curves for a Niobium HEB fabricated at the University of Virginia. *Courtesy of Lei Lui [4].*

IV. Fabrication

The size of the HEB's requires nanoscale fabrication techniques. The options available in the University of Virginia Microfabrication Laboratory (UVML) include electron-beam lithography and a recently developed procedure known as "Ti-line processing" [6]. The later approach is attractive in that it does not require direct-write processing, allows all devices to be made in parallel, and exploits 2 µm conventional lithography to yield nanoscale devices.

The Ti-line technique (fig. 7) is based on forming a thin strip of titanium suspended above a substrate to form a shadow mask. The width of the titanium line is controlled by the sputter conditions (rate and angle) under which the material is deposited. The line is formed by creating a step profile in a polyimide coating the substrate (fig. 7a). Titanium is sputtered onto the substrate, including the step sidewalls. Resist "anchors" are put on either side of the Ti-line (fig. 7b). Reactive Ion Etching (RIE) removes the flat surfaces of Ti and the underlying resist, leaving a titanium bridge suspended over the substrate. The suspended Ti-line is used as either an evaporation or an etch mask. In fabricating the HEB's for the six-port, two different Ti-lines are employed to form the length and width of the bolometer. A 200 nm wide line is used as an evaporation mask for the gold that comprises the microstrip circuit (fig. 7c). This determines the length of the HEB. All unnecessary gold is lifted off using traditional lithography. The HEB length is now defined and the Ti-line removed. A second Ti-line, perpendicular to the first, is used to define the HEB width of 100 nm (fig. 7d). This Ti-line is used as an etch mask to form the niobium bridge (fig. 7e). This etch mask is employed to remove all underlying niobium except that needed for the HEB's. Once these Ti-lines are removed, the six-port reflectometer is complete (fig. 7f).

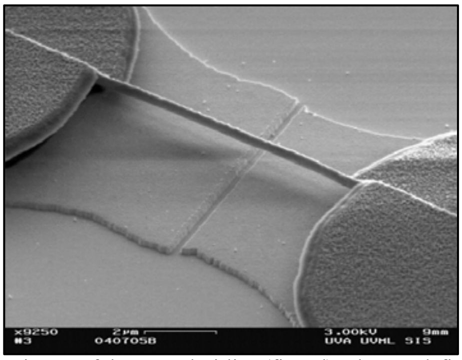

Fig. 6: SEM image of the second Ti-line (fig. 7d). The gap defines the HEB length and the Ti-line will define the HEB width. *Courtesy of J. Schultz [4]*.

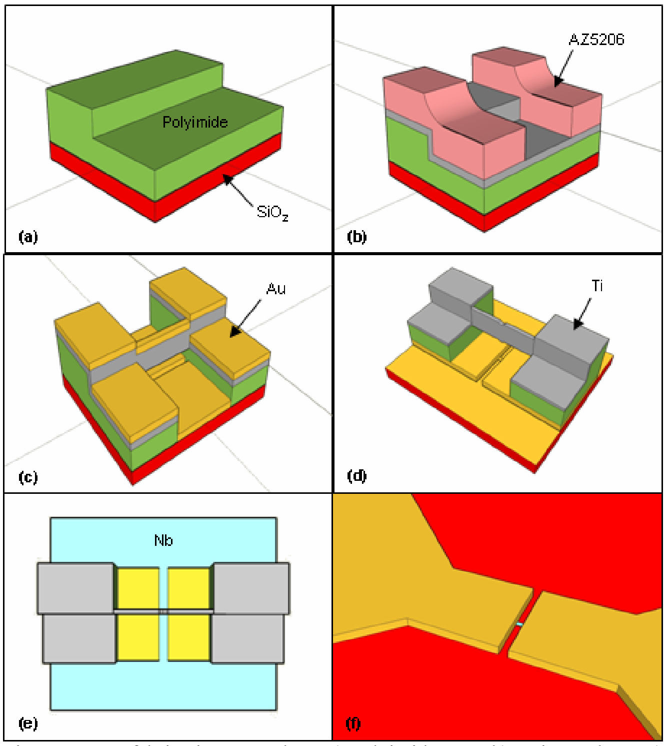

Fig. 7: HEB fabrication procedure; a) polyimide step; b) resist anchors; c) Ti-line after gold evaporation – HEB length is now defined; d) Ti-line defining HEB width; e) Ti-line as an etch mask (top view); f) final HEB. Materials are color coded as labeled.

V. Proof of Concept

The microstrip feed and antenna portion of the instrument have been independently fabricated to test the polarization concept and provide estimates for the power available to each HEB. The power available at the theoretical DUT location is measured using an Erickson Power Meter. The losses between the DUT and HEB's can be calculated and combined with the measured data to estimate the power available to each HEB. The polarization dependence is tested by rotating the annular slot structure and measuring the resulting change in power.

A. Design and Test Setup

Two different microstrip designs have been fabricated and tested (fig. 8). The first design (fig. 8a) is simply a loop of microstrip line with impedance that matches as closely as possible to the antenna impedance (110Ω). The microstrip impedance (28Ω) is determined by the fabrication tolerances and practical limits on the dielectric thickness (4000Å) and microstrip line width (2µm). The second design (fig. 8b) includes a stub tuning network to more closely match the

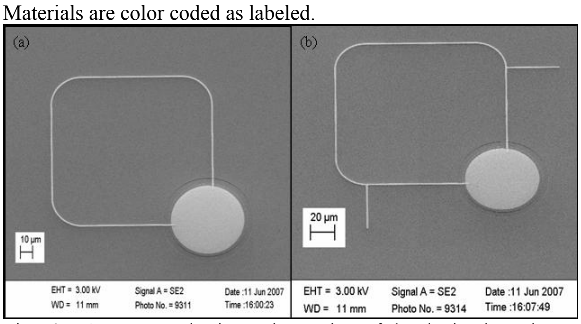

Fig. 8: Antenna and microstrip portion of the device have been fabricated independently to measure available power, validate loss calculations, and prove the polarization concept. Two designs were fabricated – (a) contains a large mismatch between the antenna and microstrip impedance; (b) utilizes a stub tuning network to address the mismatch.

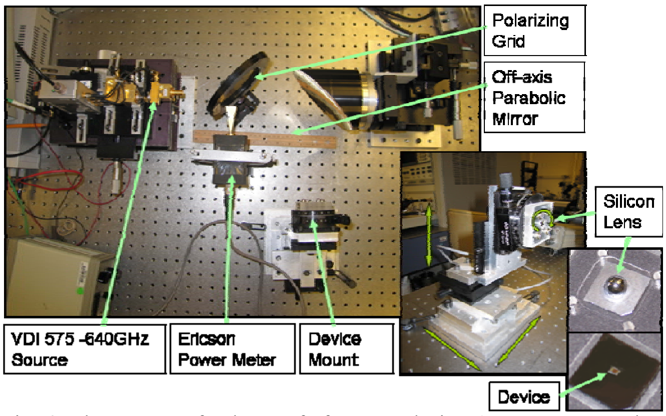

Fig. 9: The test setup for the proof-of-concept device. A VDI source sends a signal through a polarizer, off from an off-axis polarization mirror, and into the device. The device is given four axis of freedom (x, y, z, rotation) for alignment. It re-radiates the signal which now is reflected by the polarization grid and into a power meter.

antenna and microstrip impedances. Upon testing the designs, no detectable signal was measured using the network with no matching.

The test setup (fig. 9) for these measurements is a portion of the overall setup shown in fig. 3. Using this configuration helps fine tune the overall setup design. A power meter is put in place of the DUT and the "return trip" does not occur. A cryostat is unnecessary as there are no HEB's on the test chip. Lastly, to help with alignment, a mount has been improvised allowing four axis of freedom, one of which is necessary for the polarization measurements.

B. *Polarization measurements*

The polarization change is demonstrated by rotating the device and measuring the resulting power at the Erickson power meter. It is seen in fig. 10 that the power nulls occur when the orientation of the device is at odd multiples of 45º and peaks at even multiples of 45º. The variations are likely caused by stray reflections in the laboratory. The expected rotational dependence can be calculated and the data is shown to follow the expected dependence:

$$\frac{P}{P_{\max}} = \cos^2(2(\theta_{\deg} - 10)),$$

where the 10° is added to account for a misalignment between the device and the 0° point.

C. *Power and loss measurements*

The power measured with the Erickson meter varies from 3 µW at 605 GHz to 34 µW at 585 GHz. The variations at different frequencies across the bandwidth are largely accounted for by the frequency response of the source (fig. 11).

The system losses can be determined through a combination of measurement and simulation. The primary source of loss is the silicon lens used to focus the signal onto the device antenna. There is a 1.5dB reflection loss on each pass, totaling 3dB. Additionally, there are smaller losses

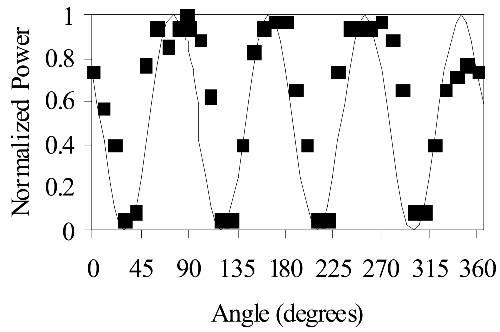

Fig. 10: The change in normalized power as the device is rotated. This shows that the polarization is being changed as expected with nulls occurring at an angle of 45°.

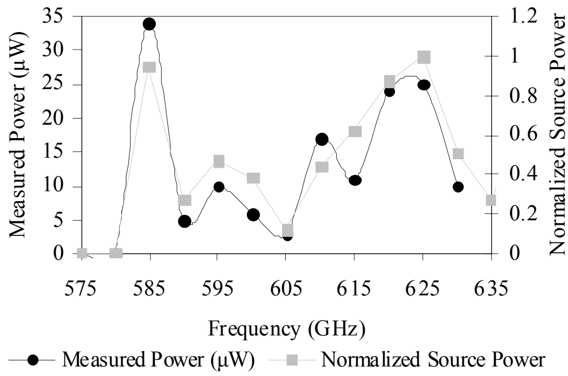

Fig. 11: The power measured in microwatts by the Erickson power meter compared to the normalized source power. The variations in measured power are a result of variations in the source.

TABLE I

POWER AVAILABLE FOR MEASUREMENT AT EACH HEB WHEN USING THE SIMULATIONS TO DETERMINE S31, S41, AND S51, AND A DUT REFLECTION COEFFICIENT OF 6DB.

	Loss (dB)	Power available (µW)
Avail. to DUT	10.8	25.2
Total losses	19.5	3.3
Coupling S31	6.3	0.79
Coupling S41	8.6	0.46
Coupling S51	6.2	0.81

predominantly from attenuation within various materials. The overall loss within this test setup is just under 9dB. Using a power available from the source of 300 µW at 585GHz gives a power available at the DUT of about 40 µW. The measured power of 34 µW agrees reasonably with these calculations.

The strong correlation between theory and measurement implies that the calculations can be applied to the final test set-up from fig. 3. Using the calculated losses through the system and assuming a DUT reflection of 6dB, the total loss is just under 20dB thus yielding an available power for coupling to the HEB's of 3.3 µW. This number can then be combined with the coupling simulation results (fig. 4) predicting values available at each HEB to be on the order of hundred's of nanowatts (table 1). These considerations determine the HEB size to be approximately 100x200nm.

CONCLUSIONS

A method for building a six-port reflectometer at submillimeter frequencies has been outlined and the design has been laid out, simulated, and is currently being fabricated. A newly developed lithography technique known as "Ti-line processing" is being employed to fabricate the nanoscale HEB's using conventional two micron lithography. A change in polarization allows a ring slot antenna to be used for both an input and measurement port. This concept has been demonstrated to agree with theory. The system losses and available power have been calculated and provide groundwork for determining the HEB size. The realization of this device will be an exciting demonstration of the ideas presented in this paper.

ACKNOWLEDGMENT

The authors thank their colleagues in the Far-Infrared Laboratory and the Microfabrication Laboratory at the University of Virginia for their advice, insight, and patience. This work is funded by the Army National Ground Intelligence Center (contract W911W5-06-C-0001) and the National Science Foundation (grant ECS-0524284).

REFERENCES

[1] G. F. Engen, "The six port reflectometer: An alternative network analyzer," *IEEE Trans. Microwave Theory Tech.*, vol. MTT-25, pp. 1075-1080, Dec. 1977.

[2] Weikle, R. M., II; Liu, Z.; Liu, H.; Liu, L.; Ulker, S.; Lichtenberger, A. W. "Six port reflectometers for terahertz scattering parameter measurements using submillimeter-wavelength detectors," *Nanofabrication: Technologies, Devices, and Applications*," vol. 5592, pp. 328-340, January 2005.

[3] G. F. Engen, "Calibrating the Six-Port Reflectometer by Means of Sliding Terminations," *IEEE Trans. Microwave Theory Tech.*, vol. MTT-26, pp. 951-957, Dec. 1978.

[4] L. Liu, "Integrated 585 GHz hot-electron bolometer mixers and focal-plane arrays for imaging applications," Ph.D. dissertation, University of Virginia, Charlottesville, VA, 2008.

[5] J. Schultz, "Superconducting hot electron bolometer terahertz mixers and related technologies," Ph.D. dissertation, University of Virginia, Charlottesville, VA, 2007.

[6] J. Schultz and A. Lichtenberger, "Investigation of Novel Superconducting Hot Electron Bolometer Geometries Fabricated with Ultraviolet Lithography," *IEEE Trans. Applied Superconductivity*, vol. 17, pp.645-648, June 2007.